ELSEVIER

Journal of Biomechanics 37 (2004) 81–88

JOURNAL OF BIOMECHANICS

www.elsevier.com/locate/jbiomech
www.JBiomech.com

A phenomenological model for estimating metabolic energy consumption in muscle contraction ☆

Lindsay J. Bhargava[a], Marcus G. Pandy[a,*], Frank C. Anderson[b]

[a] Department of Biomedical Engineering, University of Texas at Austin, ENS 610, Austin, TX 78712, USA
[b] Department of Mechanical Engineering, Biomechanical Engineering Division, Stanford University, USA

Accepted 28 May 2003

Abstract

A phenomenological model for muscle energy consumption was developed and used in conjunction with a simple Hill-type model for muscle contraction. The model was used to address two questions. First, can an empirical model of muscle energetics accurately represent the total energetic behavior of frog muscle in isometric, isotonic, and isokinetic contractions? And second, how does such a model perform in a large-scale, multiple-muscle model of human walking? Four simulations were conducted with frog sartorius muscle under full excitation: an isometric contraction, a set of isotonic contractions with the muscle shortening a constant distance under various applied loads, a set of isotonic contractions with the muscle shortening over various distances under a constant load, and an isokinetic contraction in lengthening. The model calculations were evaluated against results of similar thermal in vitro experiments performed on frog sartorius muscle. The energetics model was then incorporated into a large-scale, multiple-muscle model of the human body for the purpose of predicting energy consumption during normal walking. The total energy estimated by the model accurately reflected the observed experimental behavior of frog muscle for an isometric contraction. The model also accurately reproduced the experimental behavior of frog muscle heat production under isotonic shortening and isokinetic lengthening conditions. The estimated rate of metabolic energy consumption for walking was 29% higher than the value typically obtained from gait measurements.

Keywords: Muscle modeling; Metabolic energy; Heat; Movement simulation; Isometric; Isotonic

1. Introduction

An accurate model of muscle energetics is an important component of multi-variable models of movement, since energy minimization is often used as a criterion to predict how muscles are coordinated to accomplish a given task (Hatze and Buys, 1977; Davy and Audu, 1987; Pandy et al., 1995; Anderson and Pandy, 2001; Pandy, 2001). One approach to including energetics in a model for muscle contraction is to use a mechanistic crossbridge-based model. A natural connection between mechanics and energetics exists in this type of framework, because ATP hydrolysis is directly coupled to crossbridge cycling (Huxley, 1957). The original crossbridge model by Huxley (1957) and multiple variations on it have been shown to produce quantitatively accurate predictions of energy output compared with the energetic relationships found experimentally by Hill (1938) (Barclay, 1998; Rouhaud and Zahalak, 1992; Ma and Zahalak, 1987). These models are rigorous, physiologically based, and have provided much insight into muscle function. However, these models also require the use of many parameters whose values are uncertain, especially for human muscles (Zahalak, 1990).

A simpler approach to modeling muscle energetics is to construct an empirical model. A Hill-type muscle model is often used in elaborate movement models due to its simplicity, the availability of data on the few necessary parameters, and its relatively accurate predictions of muscle force (Zajac, 1989; Zahalak, 1990; van den Bogert et al., 1998). Unfortunately, the Hill model lacks a connection between the force-producing

☆ Please see attached supplementary material to go onto journal website.

*Corresponding author. Tel.: +512-232-5404; fax: +512-471-0616.
E-mail address: pandy@mail.utexas.edu (M.G. Pandy).

0021-9290/03/$ - see front matter © 2003 Elsevier Ltd. All rights reserved.
doi:10.1016/S0021-9290(03)00239-2

properties of muscle (mechanics) and the mechanisms underlying heat production (energetics). Several authors have taken the empirical approach to modeling muscle energetics (Hatze and Buys, 1977; Davy and Audu, 1987; Schutte et al., 1993; Anderson and Pandy, 2001). However, in these studies the energy equations were not validated against experimental data.

The purpose of this study was twofold: first, to develop an empirical model for muscle energy consumption, defined here as the transformation of chemical energy into the performance of mechanical work and the liberation of heat, that could be used in conjunction with a simple Hill-type model for muscle contraction; and second, to validate the behavior of the model against available experimental data. The objective was not to explain the processes of muscular energetics, but to reproduce the observed behavior. The model was designed to provide an easy and reliable way for researchers using complex multiple-muscle systems to estimate total energy consumption in simulations of human movement. The following questions are addressed. Can a phenomenological model of muscle energetics, based on a Hill-type model of muscle mechanics, accurately represent the total energetic behavior of frog muscle in isometric, isotonic, and isokinetic contractions? And, how does a phenomenological energetics model, which has been validated against experimental data from frog muscle, perform in a large-scale multiple-muscle model of human walking?

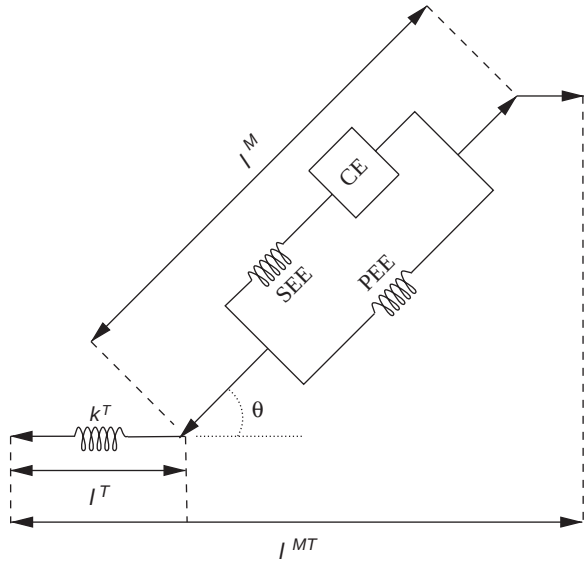

Fig. 1. Diagram of the Hill model on which the present energetics model is based. Lengths of the muscle, tendon, and musculotendon actuator are shown by l^M, l^T, and l^{MT}, respectively. CE, contractile element, models the force-producing components of the muscle characterized by the force–length and force–velocity properties. SEE, series elastic element, is a nonlinear spring representing the internal elastic components of the muscle in series with the force producing components. PEE, parallel elastic element, is a non-linear spring representing the passive elastic nature of the muscle. Tendon is represented by a linear spring with stiffness k^T. Angle of pennation, θ, is the angle formed between the lines of action of the muscle and tendon. To simulate isometric and isotonic contractions of frog sartorius muscle in vitro, tendon rest length and muscle pennation angle were both set to zero in the model. Muscle parameters used in the simulations are given in Tables 1–3.

2. Methods

According to the first law of thermodynamics, the total rate of energy consumption, $\dot{E}$, is equal to the rate at which heat is liberated, $\dot{H}$, plus the rate at which work is done, $\dot{W}$:

$$\dot{E} = \dot{H} + \dot{W}. \tag{1}$$

During muscular contraction, the amount of heat liberated is measured by the temperature change within a muscle (Hill, 1938), and, if there is also a change in length, mechanical work is done.

In this study, the total rate of muscular energy consumption was described as the sum of five terms with the rate of heat liberation being further subdivided, thus

$$\dot{E} = \dot{A} + \dot{M} + \dot{S} + \dot{B} + \dot{W}, \tag{2}$$

where $\dot{A}$ is the activation heat rate, $\dot{M}$ is the maintenance heat rate, $\dot{S}$ is the shortening heat rate, $\dot{B}$ is the basal metabolic rate, and $\dot{W}$ is the work rate (Mommaerts, 1969; Hatze and Buys, 1977; Davy and Audu, 1987; Anderson and Pandy, 2001). In particular, the phenomenological equations constructed by Anderson (1999) for these rate terms were refined to explain experimental results for the energetics of isolated frog sartorius. The necessary parameters for these equations are readily obtained from the parameters typically used to specify the mechanical properties of 3-element, Hill-type muscle models (Zajac, 1989) (see Fig. 1).

The activation heat represents the tension-independent heat liberated upon the stimulation of a muscle and is thought to be due to the movement of Ca^{++} ions (Kushmerick, 1983). The activation heat rate was represented by the sum of two terms, one term for the portion of a muscle comprised of fast twitch fibers and one for the portion comprised of slow twitch fibers:

$$\dot{A} = \phi m f_{\text{fast}} \dot{A}_{\text{fast}} u_{\text{fast}}(t) + \phi m f_{\text{slow}} \dot{A}_{\text{slow}} u_{\text{slow}}(t), \tag{3}$$

where ϕ is a decay function, m is the total mass of the muscle, f_{fast} and f_{slow} are the mass fractions of fast and slow twitch fibers in the muscle, respectively, $\dot{A}_{\text{fast}}$ and $\dot{A}_{\text{slow}}$ are the activation heat rate constants for fast and slow twitch fibers, and $u_{\text{fast}}(t)$ and $u_{\text{slow}}(t)$ are the excitation levels of the fast and slow twitch fibers. For muscle models in which only a single excitation level $u(t)$ is used to represent the recruitment of both fast and slow twitch fibers, cosine and sine functions were used to convert $u(t)$ into separate levels for $u_{\text{fast}}(t)$

and $u_{slow}(t)$:

$$u_{fast}(t) = 1 - \cos(\pi/2\ u(t)), \tag{4}$$

$$u_{slow}(t) = \sin(\pi/2\ u(t)). \tag{5}$$

Eqs. (4) and (5) together approximate the size principle of motor unit recruitment in which slow twitch fibers are recruited in preference to fast twitch fibers at low levels of excitation, and both slow and fast twitch fibers are recruited at the higher levels of excitation. The decay function ϕ models the observed time course of heat production in which most of the heat is produced early and decays with a time constant of 45 ms down to 6% of its initial level (Homsher et al., 1972):

$$\phi = 0.06 + \exp(-t_{stim}u(t)/\tau_\phi), \tag{6}$$

where τ_ϕ is the decay time constant (i.e., 45 ms), $u(t)$ is the net excitation level of the muscle, and t_{stim} is the amount of time the muscle has been excited above 10%.

The maintenance heat rate is the stable heat rate produced during isometric tetanus due to the cycling of actin–myosin crossbridges (Mommaerts, 1969; Kushmerick, 1983). The maintenance heat rate was also modeled as the sum of two terms, one for the portion of a muscle comprised of fast twitch fibers and one for the portion comprised of slow twitch fibers:

$$\dot{M} = L(\tilde{l}^M)mf_{fast}\dot{M}_{fast}u_{fast}(t) + L(\tilde{l}^M)mf_{slow}\dot{M}_{slow}u_{slow}(t), \tag{7}$$

where $L(\tilde{l}^M)$ is a function that models the dependence on muscle length and $\dot{M}_{fast}$ and $\dot{M}_{slow}$ are the maintenance heat rate constants for fast and slow twitch fibers, respectively. As a muscle shortens below its optimal fiber length (l_o^M), the maintenance heat rate decreases to approximately 50% of its peak value. As a muscle is lengthened beyond l_o^M, the maintenance heat rate decreases until at a length of $1.5l_o^M$, where there is no overlap of actin and myosin filaments, the maintenance heat rate falls to zero (Mommaerts, 1969). This length dependence was represented as a piecewise linear function of normalized muscle fiber length (Fig. 2).

The shortening heat rate is the rate at which heat is produced during a concentric or eccentric contraction beyond that which occurs during isometric contraction at the same force (Hill, 1938; Kushmerick, 1983). The shortening heat rate was found by Hill (1964) to be proportional to the velocity of shortening:

$$\dot{S} = -\alpha v_{CE}, \tag{8}$$

where α is a proportionality constant and v_{CE} is the velocity of the contractile element (positive velocity for lengthening or eccentric contraction). For concentric contractions, the proportionality constant was modeled as a function of both the isometric force of the muscle (F_{iso}^M) and the current force developed by the muscle (F^M):

$$\alpha = 0.16F_{iso}^M(a(t), l^M) + 0.18F^M; \quad v_{CE} \leqslant 0, \tag{9}$$

where F_{iso}^M is the force that would be developed at activation $a(t)$ and muscle length l^M under isometric conditions (i.e., $v_{CE} = 0$). For eccentric contractions, the shortening heat rate is negative and has a different constant of proportionality (Abbott and Aubert, 1951):

$$\alpha = 0.157F^M; \quad v_{CE} > 0. \tag{10}$$

The basal metabolic rate for resting frog skeletal muscle at 0°C was reported as 0.0225 W/kg (Rall, 1985). Therefore, the basal heat rate was given by

$$\dot{B} = 0.0225m, \tag{11}$$

where m is the mass of the muscle.

The work rate was computed as the product of the force of the contractile element (F_{CE}) and its shortening velocity (v_{CE}):

$$\dot{W} = F_{CE}(l_{CE}, v_{CE}, a(t))v_{CE}, \tag{12}$$

where F_{CE} depends on the length, shortening velocity, and activation level of the muscle.

For details concerning the model of muscle energetics, the reader is referred to the supplementary material available at the Journal of Biomechanics web site (See Webpage of the Journal of Biomechanics).

The phenomenological model of muscle energetics (i.e., Eqs. (2)–(12)) was used to predict energy consumption in simulations of isometric, isotonic shortening, and isokinetic lengthening contractions of frog sartorius muscle. Each simulation protocol was developed to duplicate an in vitro experiment as closely as possible. Tables 1–3 provide the assumed parameter values. In the isometric simulation, the muscle was held at its optimal fiber length (Curtin and Woledge, 1979). In the isotonic simulations with shortening, the muscle was initially held at optimal length and then released to shorten

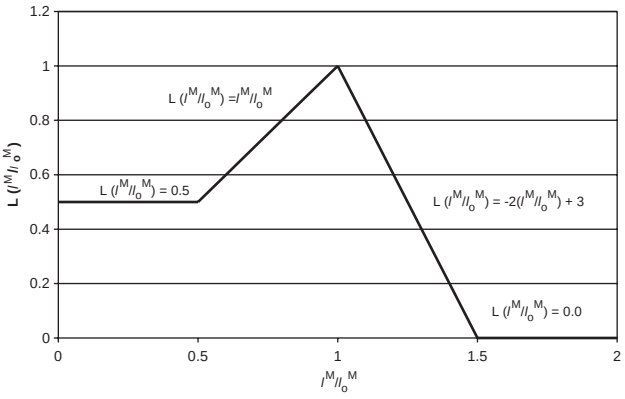

Fig. 2. Length dependence of the maintenance heat rate. The function $L(l^M/l_o^M)$ is used for approximating the maintenance heat rate $\dot{M}$ (Eq. (7)).

Table 1
Constants for activation heat rates ($\dot{A}_{fast}$ and $\dot{A}_{slow}$) and maintenance heat rates ($\dot{M}_{fast}$ and $\dot{M}_{slow}$) for slow and fast twitch muscle. Activation heat rate constants were obtained by dividing activation heats by twitch times (Mommaerts, 1969; Kushmerick, 1983; Rall, 1979; Smith, 1972; Abbott et al., 1951; Lieber, 1992). Differences in maintenance heat rate constants between the frog sartorius and human muscle are due to the temperature dependence of maintenance heat; a Q10 factor of 2.5 was assumed (i.e., for every increase in temperature of 10°C, the maintenance heat rate was increased by 2.5) (Mommaerts, 1969; Kushmerick, 1983). See supplementary information for details

	Frog sartorius (W/kg)	Human muscle (W/kg)
$\dot{A}_{fast}$	20	133
$\dot{A}_{slow}$	[a]	40
$\dot{M}_{fast}$	12	111
$\dot{M}_{slow}$	[a]	74

[a] The frog sartorius was assumed to be comprised of all fast-twitch fibers (Smith and Ovalle, 1973; Lutz et al., 1998).

Table 2
Muscle-specific parameters for frog sartorius assumed in the model. Parameters were taken from the experiments that were simulated. Symbols appearing in the table are optimal fiber length (l_o^M) and the corresponding maximum isometric force developed by the muscle (F_o^M). The average mass of the frog sartorii used by Hill (1964) was substantially larger than those used in the other experiments. Hill (1964) discussed the exceptionally high dry weight of these muscles and attributed it to the frogs being well fed and treated before delivery

	Isometric and isokinetic lengthening (Curtin, 2001)[a]	Isotonic shortening—constant load, variable distance (Hill, 1938)	Isotonic shortening—constant dist., variable load (Hill, 1964)
Mass	50.5 mg	89 mg	250 mg
l_o^M	26.9 mm	29.5 mm	34.5 mm
F_o^M	35 g	43 g	180 g

[a] Personal communication from Dr. Nancy Curtin, Imperial College, London.

Table 3
Non-specific muscle parameters for frog sartorius assumed in the model simulations. Tendon was not used in the experimental muscle preparations, so tendon slack length, l_s^T, was set to a very small value in the model. Frog sartorius muscles were assumed to be parallel fibered (McMahon, 1984) and comprised of fast twitch fibers only (amphibian types 1 and 2) (Smith and Ovalle, 1973; Lutz et al., 1998). The maximum shortening velocity for frog sartorius at 0°C, v_{max}, was obtained from Hill (1938)

Parameter	Value
l_s^T	0.01 mm
Pennation angle, θ	0°
% Fiber type	100% fast
v_{max}	2.0 muscle lengths/s

against a specified load. Two types of isotonic simulations were conducted: one under a constant load with various shortening distances (Hill, 1938), and the other under various loads with a constant shortening distance (Hill, 1964). In the lengthening simulation, the muscle was initially held for isometric contraction at a length below its optimal fiber length, and then was stretched at a pre-determined constant velocity. This simulation protocol was based on the procedures reported by Cole et al. (1996). In all isolated muscle simulations, the muscle was stimulated maximally.

Finally, to evaluate the generalized applicability of the phenomenological model of muscle energetics, we implemented it in a complex multiple-muscle simulation of human walking (Anderson and Pandy, 2001), and compared the results to experimental data for energy consumption during level walking. The results differ from the results previously reported by Anderson and Pandy (2001) primarily due to the addition of the decay function ϕ in the activation heat rate (Eq. (3)) and due to the distinction in the shortening heat rate made between concentric and eccentric contractions (Eqs. (9) and (10)).

3. Results

The total energy estimated by the model accurately reflected the observed experimental behavior of frog muscle for an isometric contraction (Fig. 3). The model produced a total of 150.2 mJ/g during a 10-s tetanus. The steady rate of heat production in the model (after 1.2 s) was approximately 13.3 mW/g.

The model also accurately reproduced the experimental behavior of frog muscle heat production under

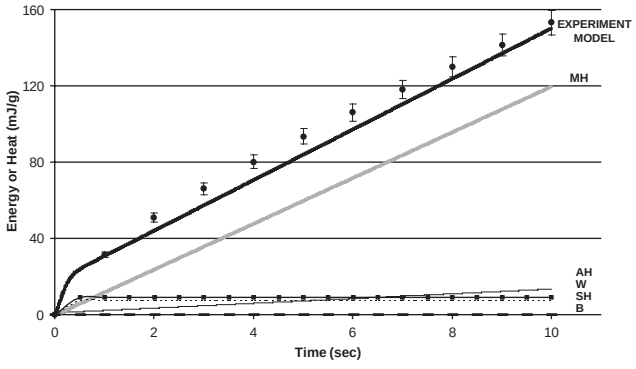

Fig. 3. Total energy consumption of frog sartorius for a 10-s isometric contraction. Model total energy results (top curve) are compared to experimental data (circles) from Curtin and Woledge (1979). Bars represent ±1 SD. The experiment measured the total energy output (heat + work) for an isometric contraction at optimal muscle length for frog (*R. temporaria*) sartorius at 0°C. Also shown are the model results for total energy breakdown into the various components of heat and work. MH, maintenance heat; AH, activation heat (solid line; W, work done (thin solid line with squares); SH, shortening heat (dotted line); B, basal heat at rest (dashed line).

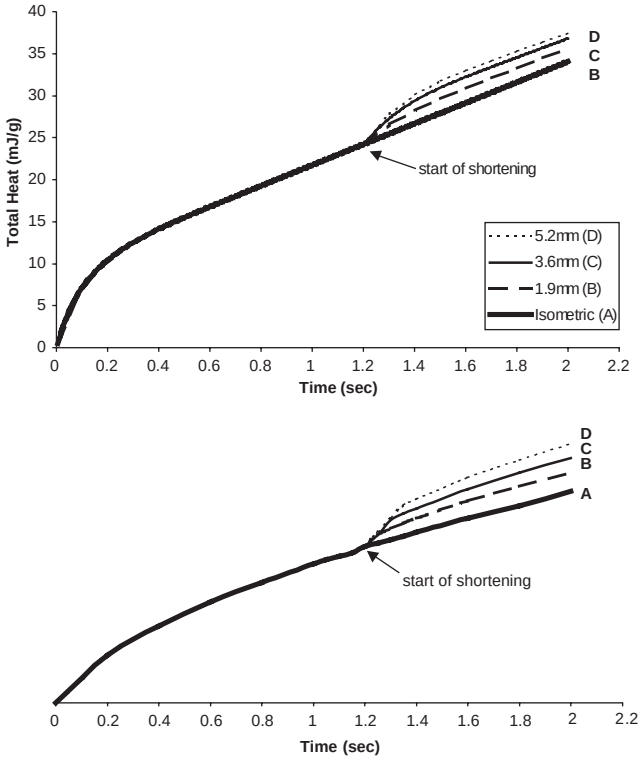

Fig. 4. Heat production in isotonic contraction of frog sartorius. Shortening distances are the same for both graphs (A = isometric, B = 1.9 mm, C = 3.6 mm, D = 5.2 mm). The top graph shows the model results for the total heat produced with various shortening distances under a 3.0 g applied load. The muscle is released from its isometric state after 1.2 s. The bottom graph, reproduced from Hill (1938), shows qualitatively the experimental results obtained from isotonic contractions on frog (*R. temporaria*) sartorius at 0°C. The experiment measured the heat produced while shortening over different distances under a constant load of 3.0 g, applied after 1.2 s of isometric contraction. No scale was reported for the vertical axis, which represents total heat produced.

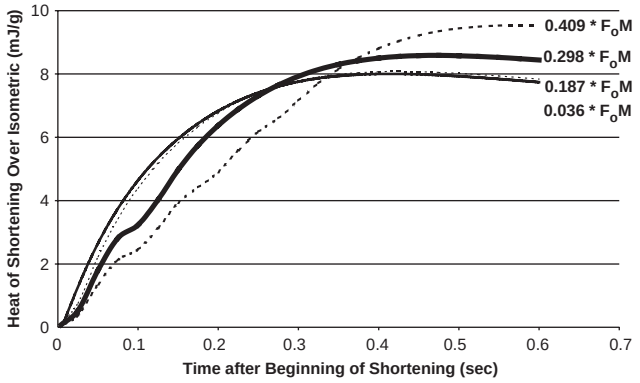

Fig. 5. Model predictions for heat of shortening over isometric ($H_{short} = H_{total} - H_{iso}$) for isotonic contractions of frog sartorius at 0°C. In each case, the model muscle shortened a fixed distance of 7 mm under the following applied loads: $0.036F_o^M, 0.187F_o^M, 0.298F_o^M$, and $0.409F_o^M$, where F_o^M is the maximum isometric force in muscle measured at its optimal fiber length. Time $t = 0$ represents the beginning of shortening. The simulations replicated an experiment performed by Hill (1964), where heat production was measured from frog (*R. temporaria*) sartorius at 0°C while the muscle shortened a constant distance of 7 mm under the loads given above. In both the experiment and the simulations, the muscle was released after 0.45 s of isometric contraction, when the tension developed had reached its maximum (Hill, 1964).

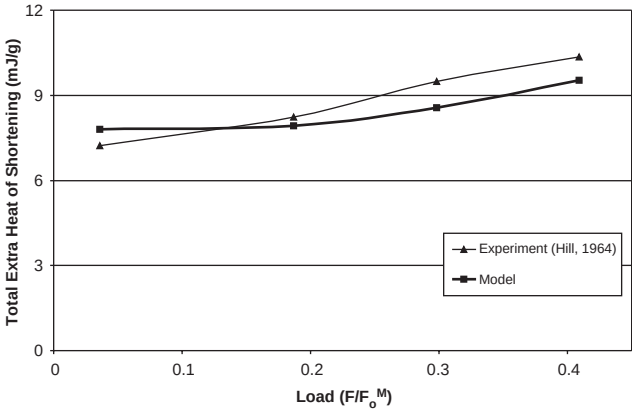

Fig. 6. Model and experimental results for total shortening heat production versus applied load for isotonic contractions of frog sartorius with shortening distance held fixed at 7 mm (cf. Fig. 5). The experiments were performed by Hill (1964), who measured heat produced from frog (*R. temporaria*) sartorius at 0°C during shortening under different loads with constant shortening distance (7 mm). Total shortening heat was taken as the amount of heat produced (over isometric) 0.3 s after shortening ended (Hill, 1964). In both the model and the experiments, applied load (abscissa) is normalized by maximum isometric force, F_o^M, developed by the muscle.

isotonic shortening conditions (Figs. 4–6). The relationship predicted by the model showed a dependence on heat with shortening distance, where the increase in the total heat between trials was in proportion to the difference in the distance shortened (Fig. 4). For example, the smallest increase in heat (0.52 mJ/g) occurred between the two trials with the smallest difference in shortening (5.2–3.6 mm = 1.6 mm) (Fig. 4, compare traces C and D). The rate of heat production increased abruptly at the onset of shortening, then slowly returned to the original steady rate within about 0.3 s after shortening ended. The model also predicted an increase in total shortening heat with load for isotonic contractions with the same shortening distance (Fig. 5). The initial rates of heat development at the start of shortening decreased with increasing load, but the total amount of shortening heat increased (Fig. 6).

The model predicted a decrease in heat production due to isokinetic lengthening (Fig. 7). The total heat produced during an isometric contraction at the starting length of simulation (i.e., 6 mm below the optimal fiber length) was greater than that produced during contraction with lengthening. After a stretch of 4 mm ($t = 3.4$ s), the total heat decreased by approximately 5% of the isometric value.

Finally, the phenomenological model performed reasonably well in a three-dimensional model of normal

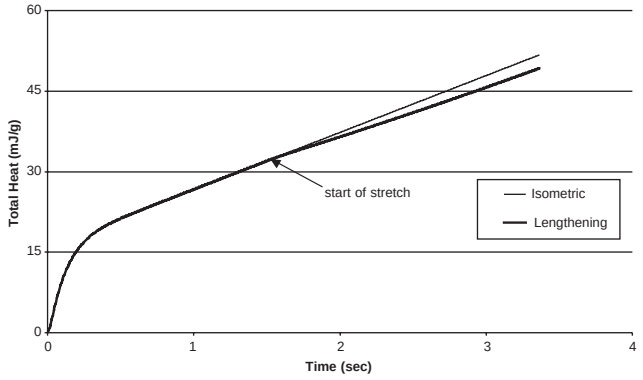

Fig. 7. Total heat produced during isokinetic lengthening. The muscle was held isometrically for 1.5 s to develop maximum tension. As in Cole et al. (1996), the starting length was l_o^M—6 mm, and the muscle was then stretched 4 mm at a rate of 4%v_{max}, ending at 3.4 s. Isometric heat shown is for muscle held at the initial length (l_o^M—6 mm). Muscle parameters used were identical with those in the experiment of Curtin and Woledge (1979).

human walking. The predicted rate of energy consumption was 5.8 W/kg at a walking speed of approximately 1.36 m/s.

4. Discussion

To address the need for a simple model that incorporates both the mechanical and energetic behaviors of muscle contraction, we developed a model of muscle energetics that is compatible with Hill-type muscle models. Although mechanistic crossbridge models have proven their accuracy in calculating muscle energetics, the use of these models in human movement studies is rare because of their complexity and the limited availability of the many required parameters. Our energetics model can be easily incorporated into the Hill-type muscle models of large-scale multiple-muscle systems to enhance the scope of information that can be obtained from simulations of movement.

A fundamental limitation of the model is that the energy rate equations are empirical, lacking a direct connection to the molecular basis of muscle contraction. The separation of metabolic heat production into components is merely a phenomenological assumption. Indeed, it is still not known exactly what processes are responsible for each element of heat production, or even if these processes can really be represented by independent terms.

This limitation is evident in the predicted breakdown of the total energy produced in an isometric contraction (Fig. 3). In the model, total activation heat comprised only 9% of the total heat produced after 10 s, whereas it has been reported to contribute between 27% and 40% of the total heat (energy-work) production of frog muscle in a tetanic isometric contraction at 0°C (Homsher et al., 1972; Homsher and Kean, 1978). It is reasonable that the maintenance heat rate was the largest component, because the muscle was maintaining a high-tension value during the isometric contraction. However, the total stable rate of heat production of 13.3 mW/g predicted by the model is within the range reported in the literature for frog sartorius at 0°C (11.5 mW/g, Curtin and Woledge (1979); 13.5 mW/g, Table 4.IV in Woledge et al. (1985); and 15.7 mW/g, Mommaerts (1969)). This suggests that the maintenance heat rate may be overestimated, since the activation heat rate is underestimated as described above (Fig. 3, MH and AH). Unfortunately, there is no clear way to reconcile this apparent anomaly in the model. To our knowledge, no experimental data are available to show the separate contributions of activation heat and maintenance heat in a force-producing tetanus, so the model calculations cannot be evaluated more precisely in this respect.

The remaining components of the predicted total energy production were more consistent with reported data. The model estimated that 9.1 mJ/g of internal work was done during the isometric contraction. Internal work refers to the early work done by the contractile elements within the muscle to stretch the elastic elements without changing the length of the entire musculotendon complex. Approximately 2 mJ/g of internal work was measured for frog sartorius at 0°C during a 10-s tetanus (Homsher and Kean, 1978). This is a relatively large difference, however, the performance of work represents only 6% of the total energy produced in the model. Therefore, this difference should have very little effect on the total energy estimate (Fig. 3, compare W and model). The work done and the shortening heat were both small in the model, because during an isometric contraction only a small amount of internal shortening occurs early in the contraction. Conforming to this behavior, the work and shortening heat rates were fairly large during the first second of contraction, but decreased to a rate near zero for the remainder of the time. Also predictably, the constant basal metabolic energy rate added a relatively insignificant amount of heat to the total energy produced.

Overall, the total energy predicted by the model was analogous to the observed energetic behavior of frog muscle in isometric contraction. Our model underestimated the energy produced after a 10-s tetanus by 2.9 mJ/g, which is approximately 2% of the experimental value (Curtin and Woledge, 1979). A correlation coefficient of $R^2 = 0.984$ reflects a good agreement between the two curves (Fig. 3).

The isotonic simulations showed that the relationship between heat and shortening distance predicted by the model was comparable to that found by Hill (1938) experimentally (Figs. 4–6). Under a constant load, for example, as the total shortening distance increased, the

total heat produced also increased (Fig. 4). A constant load resulted in a fairly constant shortening velocity, which resulted in a constant shortening heat rate across trials. Thus, as the shortening distance increased, the muscle simply shortened for a longer period of time, and a proportionally larger amount of shortening heat was produced.

The model's predicted increase in total shortening heat with load was comparable to experimental observations by Hill (1964). The comparison between the magnitudes of total shortening heat for the different loads from Hill (1964) and those produced by the model (Fig. 6) shows that the trend is the same, although the model overestimated heat production for small loads and underestimated it for large loads. The difference was fairly small, however, ranging from 0.32 mJ/g (4%) at $0.187F_o^M$ to 0.94 mJ/g (10%) at $0.298F_o^M$. With a constant shortening distance, an increase in load caused a decrease in shortening velocity, leading to a longer period of shortening time. Slower velocities caused the heat rate to decrease with load (see Eqs. (8) and (9)), but the extended shortening time resulted in a larger total heat after shortening ended.

For the isokinetic lengthening simulation (Fig. 7), the decrease in heat shown by the model (5%) was similar to the decrease reported by Abbott and Aubert (1951) (5.7%) for frog muscle undergoing very slow stretches ($0.5\%v_{max}$). This must be considered as a qualitative comparison, however, because the simulation we performed was not identical with the experiment reported by Abbott and Aubert (1951). We simulated stretch at lengths below the optimal fiber length (l_o^M) and at a speed of $4\%v_{max}$, whereas data reported by Abbott and Aubert (1951) are for stretches with the muscle held at lengths above l_o^M and stretched at $0.5\%v_{max}$. We did not simulate lengthening beyond l_o^M because the behavior of the Hill model is known to be unreliable for lengthening in this range (Cole et al., 1996).

The estimated rate of metabolic energy consumption for walking was 5.8 W/kg, 29% higher than the experimental value. Experimental results show that humans use on average 4.5 W/kg when walking at a freely selected cadence and speed (1.36 m/s) (Burdett et al., 1983). There are two possible explanations for this difference. First, measurements of metabolic energy expenditure reported in the literature are for walking with arm swing (Burdett et al., 1983). Since the walking model used here represented the head, arms, and torso as a single rigid body (Anderson and Pandy, 2001), it could not benefit from any improvement in metabolic energy consumption that may arise from relative motion of the torso and arms. Ralston (1965) found that immobilization of the torso and arms increases energy expenditure by roughly 10%, so neglecting the relative movements of the torso and arms accounts at least in part for the elevated estimate of metabolic energy obtained from the model. Higher estimates of energy consumption in the model may also be due to the values assumed for the energetic parameters that appear in the rate equations, specifically the amount of activation heat produced during a twitch and the maintenance heat rate during tetanus. Values of these parameters used in the simulation of walking were based on data reported for frog muscle, not human muscle (see Table 1). Thus, future attempts to improve the model's predictive capability in terms of human activity should focus on using accurate values of activation and maintenance heat derived for human skeletal muscle.

Creating a simple, yet precise model of muscle energetics to aid the study of complex three-dimensional human movement is challenging. There is difficulty in obtaining model parameters appropriate for healthy human skeletal muscle. Also, experiments performed on isolated muscle typically do not mimic the conditions present during activity. A key to refining the equation for activation heat is to understand how it is liberated during sustained, submaximal contractions, not just during twitches. Indeed, the individual behaviors of the activation and maintenance heat components are facets of metabolic energy consumption that must be elucidated by experiment before refinements can be made and more conclusive validations undertaken on this type of phenomenological model.

Although our model of muscle energetics is simple, it does make predictions that are in good qualitative agreement with experiment and can, therefore, serve as a starting point for characterizing the metabolic activity of muscles during movement. The apparent discrepancy between model and experiment in the proportions of activation and maintenance heat liberated during a contraction does not denigrate the value of the model, because its purpose was not to explain the individual processes of muscle heat production. The value of the model rests with the fact that it is relatively simple and computationally inexpensive, the values of its parameters are readily obtained from experiment, and it produces a reasonable estimate of the total energy consumed during a contraction.

References

Abbott, B., Aubert, X., 1951. Changes of energy in a muscle during very slow stretches. Proceedings of the Royal Society of London, Series B, Biological Sciences 139, 104–117.

Abbott, B., Aubert, X., Hill, A., 1951. The absorption of work by a muscle stretched during a single twitch or a short tetanus. Proceedings of the Royal Society of London, Series B, Biological Sciences 139, 86–104.

Anderson, F.C., 1999. A dynamic optimization solution for a complete cycle of normal gait. Ph.D Thesis, The University of Texas at Austin, Austin, TX.

Anderson, F., Pandy, M., 2001. Dynamic optimization of human walking. Journal of Biomechanical Engineering 123, 381–390.

Barclay, C., 1998. A weakly coupled version of the Huxley crossbridge model can simulate energetics of amphibian and mammalian skeletal muscle. Journal of Muscle Research and Cell Motility 20, 163–176.

Burdett, R., Skrinar, G., Simon, S., 1983. Comparison of mechanical work and metabolic energy consumption during normal gait. Journal of Orthopedic Research 1, 63–72.

Cole, G., van den Bogert, A., Herzog, W., Gerritsen, K., 1996. Modelling of force production in skeletal muscle undergoing stretch. Journal of Biomechanics 29, 1091–1104.

Curtin, N., Woledge, R., 1979. Chemical change and energy production during contraction of frog muscle: how are their time courses related? Journal of Physiology 288, 353–366.

Davy, D., Audu, M., 1987. A dynamic optimization technique for predicting muscle forces in the swing phase of gait. Journal of Biomechanics 20, 187–201.

Hatze, H., Buys, J., 1977. Energy-optimal controls in the mammalian neuromuscular system. Biological Cybernetics 27, 9–20.

Hill, A.V., 1938. The heat of shortening and the dynamic constants of muscle. Proceedings of the Royal Society of London, Series B, Biological Sciences 126, 136–195.

Hill, A.V., 1964. The effect of load on the heat of shortening of muscle. Proceedings of the Royal Society of London, Series B, Biological Sciences 159, 297–318.

Homsher, E., Kean, C., 1978. Skeletal muscle energetics and metabolism. Annual Reviews in Physiology 40, 93–131.

Homsher, E., Mommaerts, W., Ricchiuti, N., Wallner, A., 1972. Activation heat, activation metabolism and tension-related heat in frog semitendinosus muscles. Journal of Physiology 220, 601–625.

Huxley, A., 1957. Muscle structure and theories of contraction. Progress in Biophysics and Biophysical Chemistry 7, 255–318.

Kushmerick, M., 1983. Energetics of muscle contraction. In: Peachey, L., Adrian, R., Geiger, S. (Eds.), Handbook of Physiology. American Physiological Society, Bethesda, MD, pp. 189–236.

Lieber, R., 1992. Skeletal Muscle Structure and Function: Implications for Rehabilitation and Sports Medicine. Williams and Wilkins, Baltimore, MD.

Lutz, G., Bremmer, S., Lajevardi, N., Lieber, R., Rome, L., 1998. Quantitative analysis of muscle fiber type and myosin heavy chain distribution in the frog hindlimb: implications for locomotory design. Journal of Muscle Research and Cell Motility 19, 717–731.

Ma, S., Zahalak, G., 1987. A simple self-consistent distribution-moment model for muscle: chemical energy and heat rates. Mathematical Biosciences 84, 211–230.

McMahon, T., 1984. Muscles, Reflexes, and Locomotion. Princeton University Press, Princeton, NJ.

Mommaerts, W., 1969. Energetics of muscular contraction. Physiological Reviews 49, 427–508.

Pandy, M., 2001. Computer modeling and simulation of human movement. Annual Review of Biomedical Engineering 3, 245–273.

Pandy, M., Garner, B., Anderson, F., 1995. Optimal control of non-ballistic muscular movements: a constraint-based performance criterion for rising from a chair. Journal of Biomechanical Engineering 117, 15–26.

Rall, J., 1979. Effects of temperature on tension, tension-dependent heat, and activation heat in twitches of frog skeletal muscle. Journal of Physiology 291, 265–275.

Rall, J., 1985. Energetic aspects of skeletal muscle contraction: implications of fiber types. Exercise and Sport Science Reviews 13, 33–74.

Ralston, H., 1965. Effects of immobilization of various body segments on the energy cost of human locomotion. Ergonomics Supplement 53, 39–46.

Rouhaud, E., Zahalak, G., 1992. The variation of isometric energy rates with muscle length: a distribution-moment model analysis. Journal of Biomechanical Engineering 114, 542–546.

Schutte, L., Rodgers, M., Zajac, F., Glaser, R., 1993. Improving the efficacy of electrical stimulation-induced leg cycle ergometry: an analysis based on a dynamic musculoskeletal model. IEEE Transactions on Rehabilitation Engineering 1, 109–125.

Smith, I., 1972. Energetics of activation in frog and toad muscle. Journal of Physiology 220, 583–599.

Smith, R., Ovalle, W., 1973. Varieties of fast and slow extrafusal muscle fibres in amphibian hind limb muscles. Journal of Anatomy 116, 1–24.

van den Bogert, A., Gerritsen, K., Cole, G., 1998. Human muscle modelling from a user's perspective. Journal of Electromyography and Kinesiology 8, 119–124.

Woledge, R., Curtin, N., Homsher, E., 1985. Energetic aspects of muscle contraction. Monographs of the Physiological Society 41, 1–357.

Zahalak, G., 1990. Modeling muscle mechanics (and energetics). In: Winters, J., Woo, S.L.-Y. (Eds.), Multiple Muscle Systems: Biomechanics and Movement Organization. Springer, New York, pp. 1–23.

Zajac, F.E., 1989. Muscle and tendon: properties, models, scaling, and application to biomechanics and motor control. In: Bourne, J. (Ed.), CRC Critical Reviews in Biomedical Engineering, Vol. 19, CRC Press, Boca Raton, pp. 359–411.